

Article

Population Dynamics of Three Polyplacophora Species from the Aegean Sea (Eastern Mediterranean)

Anastasios Varkoulis, Konstantinos Voulgaris *, Daniil Solonas Zachos and Dimitris Vafidis

Department of Ichthyology and Aquatic Environment, University of Thessaly, Nea Ionia, 38445 Volos, Greece; avarkoulis@uth.gr (A.V.); dazachos@uth.gr (D.S.Z.); dvafidis@uth.gr (D.V.)

* Correspondence: kvoulgaris@uth.gr

Abstract: The present study is the first to examine spatio-temporal variations in the densities and morphometrics of three shallow water Polyplacophora species (*Rhyssoplax olivacea*, *Acanthochitona fascicularis* and *Lepidopleurus cajetanus*), native to the eastern Mediterranean, while also estimating several growth parameters. Two intertidal boulder fields located in the Pagasitigos gulf (central Aegean) were sampled monthly with SCUBA diving using quadrant sampling, to compare the spatial and temporal (month, season) effects on their size, population density and dispersion pattern. Region was the most significant factor influencing the abundance and size for all three species, while the temporal scales affected mostly *Rhyssoplax olivacea*. The effect of a boulder under the surface was only significant for the density of *Lepidopleurus cajetanus*. The standardized major axis method showed that the three species exhibited different allometric relationships between length, width and weight, while a slope comparison between regions yielded significant, in most cases, results. Using the standardized Morisita index for dispersion, a clustered pattern was observed for all species seasonally, with the exception of *Acanthochitona fascicularis* in Plakes in autumn and winter. To estimate the growth parameters, a bootstrapped Electronic Frequency Analysis (ELEFAN) utilizing a genetic algorithm was employed on pooled populations. L_{∞} and K varied among the three species with *A. fascicularis* exhibiting the highest L_{∞} and *L. cajetanus* the lowest K value.

Keywords: abundance; allometry; dispersion; growth; boulder field



Citation: Varkoulis, A.; Voulgaris, K.; Zachos, D.S.; Vafidis, D. Population Dynamics of Three Polyplacophora Species from the Aegean Sea (Eastern Mediterranean). *Diversity* **2023**, *15*, 867. <https://doi.org/10.3390/d15070867>

Academic Editors: Bert W. Hoeksema, Andrea De Felice and Iole Leonori

Received: 15 May 2023

Revised: 10 July 2023

Accepted: 11 July 2023

Published: 18 July 2023



Copyright: © 2023 by the authors. Licensee MDPI, Basel, Switzerland. This article is an open access article distributed under the terms and conditions of the Creative Commons Attribution (CC BY) license (<https://creativecommons.org/licenses/by/4.0/>).

1. Introduction

Polyplacophora are mollusks typically found in midlitoral and shallow sublitoral boulder fields [1]. They are considered grazers, possibly stabilizing the barrens created by sea urchins [2]. Their bioerosive potential has also been established and is comparable to other important bioeroders [3]. There is extensive literature on a variety of organisms inhabiting this zone in the eastern Mediterranean [4,5]. Data regarding the presence of chiton species in the eastern Mediterranean are rather scarce and no studies exist regarding the spatio-temporal variations of distribution and abundance [6,7].

The patterns of distribution have been shown to be substantially different in a spatial scale, ranging from some centimeters to hundreds of meters, regarding intertidal mollusks [8]. Temporally, the dispersion pattern of these organisms can significantly change seasonally, but also over longer periods of time [9,10]. A number of studies have investigated the influence of a variety of abiotic and biotic factors, mainly along the Pacific and Atlantic coasts, where it was evident that more data would be essential for a better understanding of the ecological aspects of Polyplacophora [11,12].

Growth parameters estimates are ecologically important in that they provide insights regarding the trophic interactions of different trophic levels. Although most species of chitons are relatively long-lived and exhibit slow growth (e.g., *Plaxiphora aurata* in Argentina with a longevity of 6–7 years, $K = 0.359$), these results may be biased towards studies of species with larger sizes [13–15]. Growth, amongst other life history features, is strongly

influenced by temperature [16]. The plasticity of the growth parameters of *Chiton articulatus* in response to global warming thermal events has already been observed [17]. Other abiotic and biotic factors might also influence these parameters, such as depth, body condition and latitude, thus leading to differences between populations of the same species [15,18–20].

This is the first study to examine the spatio-temporal effects on dispersion and abundance and to estimate the growth parameters for three co-occurring intertidal and shallow subtidal Polyplacophora species of the Eastern Mediterranean Sea. The present study will serve as a steppingstone for further research, possibly on the density dependent effects of these organisms on midlittoral and shallow sublittoral ecosystems. This will be particularly important in the future, since these ecosystems are expected to be notably susceptible to ocean acidification.

2. Materials and Methods

2.1. Field Sampling

The present study was carried out in two shallow subtidal boulder fields (20 m × 100 m) in the Pagasitikos Gulf (central Aegean, Hellas), namely in the regions Agios Stefanos (AS; 39°18'21" N, 22°56'23" E) and Plakes (PL; 39°20'57" N, 22°57'55" E). These two regions are considered semi-enclosed bights with relative protection from wave action. Monthly samplings were performed in both regions from April 2022 to April 2023. Five replicate quadrat plots (1 m × 1 m) were haphazardly placed at each site and all polyplacophoran specimen were collected with SCUBA diving at depths between 1 and 2 m.

2.2. Selection of Species and Morphometric Measurements

Prior to morphometric measurements, a relaxation protocol was followed, consisting of gradual changes of sea to fresh water (until 1:1), while also adding a few drops of 10% ethanol [21]. Specimens were then classified to species level, using the relative literature [6,7]. The species examined in the present study were *R. olivacea*, *A. fascicularis* and *L. cajetanus*, due to their constant presence (Figure 1). In Agios Stefanos, a very small number of *Ischnochiton rissoi* and *Acanthochitona crinita* was occasionally observed, but these species were not included in the present study. Total length and width were measured using a vernier caliper (± 0.01) and wet weight was measured using a digital balance to the nearest 0.0001 g. Individuals were first measured and were subsequently stored in sample containers in the laboratory museum. ImageJ software (v 1.54d; [22]) was used to measure the undersurface of each boulder.

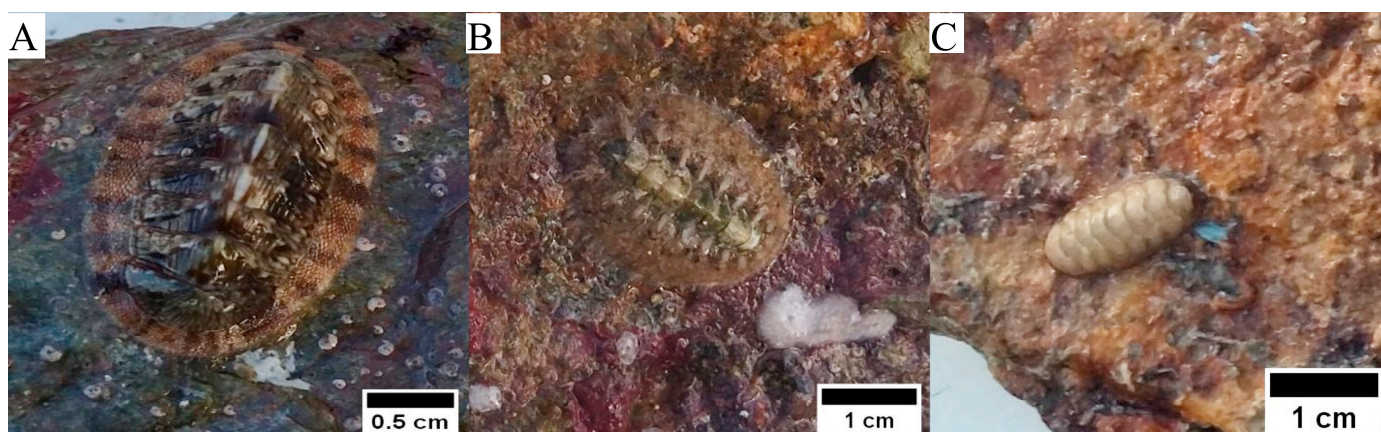


Figure 1. Photographs of the three examined species on the undersurface of boulders. (A) *Rhysoplax olivacea*, (B) *Acanthochitona fascicularis* and (C) *Lepidopleurus cajetanus*, Agios Stefanos, Pagasitikos Gulf, Central Aegean Sea (photo by D.S. Zachos, 25 November 2022).

2.3. Data Analysis

All statistical analyses were carried out using R studio (ver. 4.0.0, R Foundation for Statistical Computing, Vienna, Austria. Accessed on 12 April 2023, from <https://www.r-project.org/>). Morphometric relationships, i.e., Length/Width, Weight/Length and Weight/Width, were estimated using the power function ($\text{Length} = a\text{Width}^b$ which equals to $\text{Log}(\text{Length}) = \log a + b\text{Log}(\text{Width})$, $\text{Weight} = a\text{Length}^b$ which equals to $\text{Log}(\text{Weight}) = \log a + b\text{Log}(\text{Length})$ and $\text{Weight} = a\text{Width}^b$ which equals to $\text{Log}(\text{Weight}) = \log a + b\text{Log}(\text{Width})$) and applying a standardized major axis estimation. Unlike in linear regression models, sma not only determines the minimum distance between the measured value and fitted curve, but also considers the deviation of the measured value for the fitted curve between both x and y directions, making it more suitable for a slope estimation of the allometric scaling equation. The association degree between the variables was calculated by the determination coefficient (R^2), while a *t*-test with a confidence level of 95% was applied to detect whether the relative growth rates of the chitons' biometric characters were isometric ($H_0: b = 1$ for Length/Width or $b = 3$ for Weight/Length and Weight/Width) or allometric ($H_1: b \neq 1$ for Length/Width or $b \neq 3$ for Weight/Length and Weight/Width). The standardized major axis estimation was conducted using the package "smatr", which can test for the heterogeneity of the slopes of different equations [23].

Data were initially tested for normality (Shapiro–Wilk test) and homogeneity (Levene test). To determine the effect of surface, season and region on the density of each species, a two-way nested ANCOVA was employed with region (two levels) and season (four levels) as fixed factors, month as the nested factor and surface as the continuous covariate, while the region–season and region–month interactions were also examined. A two-way nested ANOVA was used to determine the intraspecific differences in morphometrics with region and season treated as fixed factors and month as a nested factor. The dispersion of each species was determined using the vegan R package and the dispindmorisita function was applied for the estimation of the Morisita index of dispersion combined with a chi-squared test. The scaled Morisita index was used ($-1 \leq \text{Imst} \leq 1$), with random distribution ranging from -0.5 to 0.5 [24].

The R package TropFishR was used to estimate the growth parameters for the three species in each region [25]. The ELEFAN method allows for estimations of the parameters from the von Bertalanffy growth function from the progression of LFQ modes (length–frequency modes) through time [26]. Following the "reconstruction" of LFQ data, a bootstrapped ELEFAN with a genetic algorithm optimization function (bootstrapped ELEFAN_GA) was applied, to assess uncertainties around the growth estimates [27]. Length bins were chosen using the empirical equation $\text{length bin} = 0.3 L_{\max}^{0.6}$, where L_{\max} is the maximum observed length [28]. The seasonally oscillating VBGF model was used, with L_{∞} the asymptotic length, K the annual growth rate, t_{anchor} the time point that corresponds to peak spawning month ($0 \leq t_{\text{anchor}} \leq 1$), Φ' the growth performance index as defined by [29], C indicating the amplitude of seasonal growth oscillation, with $0 \leq C \leq 1$ ($C = 0$ indicates constant growth and $C = 1$ indicates seasonal cessation of growth) and the summer point t_s , which is the fraction of the year where growth is considered to be maximum [30]. The value for t_0 was estimated using the smallest observed length for each species, by considering it as L_0 in the von Bertalanffy equation [31]. The determination of the moving average (MA) followed the rule of thumb, which uses the approximate number of bins spanning the smallest length–frequency width of the LFQ data [25]. The settings for precision-optimized ELEFAN_GA were maxiter = 50, run = 10 and popSize = 60, with 200 bootstrap runs. Values for age corresponding to length were obtained using the VBGF function from TropFishR. Data were then fitted in linear growth curves using the ordinary least squares method.

3. Results

3.1. Density and Morphometrics

R. olivacea was the most abundant out of the three examined species, while *A. fascicularis* and *L. cajetanus* exhibited similar densities (Figure 2). The three species appear to differ

regarding their morphometrics, with *R. olivacea* being largest, while *L. cajetanus* exhibits the smallest values for the three variables (Table 1, Figure 2).

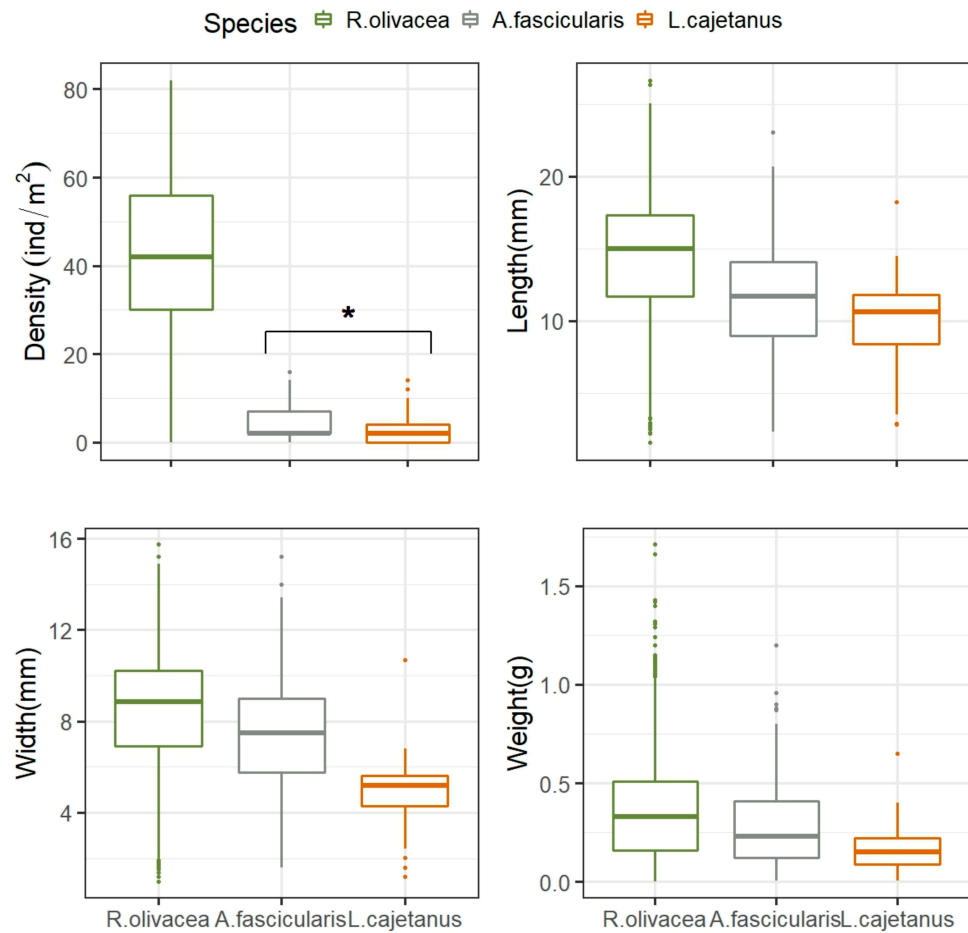


Figure 2. Boxplots showing interspecific differences in density and morphometrics for the three examined species. Dots indicate outliers, while asterisks (*) denote similarities.

Table 1. Spatial and seasonal mean values and standard deviation regarding the morphometric measurements and population density for the three studied species.

		Length (mm)	Width (mm)	Weight (g)	Density (ind/m ²)
<i>R. olivacea</i>	Agios Stefanos	15.06 ± 4.43	8.88 ± 2.56	0.42 ± 0.28	33.8 ± 17.54
	Plakes	13.45 ± 4.44	7.95 ± 2.62	0.31 ± 0.22	44.76 ± 18.58
	Spring	14.42 ± 4.91	8.57 ± 2.91	0.37 ± 0.26	48.78 ± 20.62
	Summer	13.84 ± 4.16	8.19 ± 2.43	0.31 ± 0.21	39.52 ± 18.08
	Autumn	13.44 ± 4.02	7.88 ± 2.39	0.32 ± 0.24	33.35 ± 16.09
	Winter	14.9 ± 4.5	8.72 ± 2.52	0.44 ± 0.29	35.63 ± 17.82
<i>A. fascicularis</i>	Agios Stefanos	12.08 ± 3.63	7.64 ± 2.3	0.3 ± 0.22	7.8 ± 6.64
	Plakes	10.5 ± 3.29	6.93 ± 2.41	0.23 ± 0.18	4.61 ± 4.71
	Spring	11.7 ± 3.64	7.45 ± 2.31	0.28 ± 0.21	11.65 ± 7.49
	Summer	11.24 ± 3.46	7.45 ± 2.63	0.24 ± 0.18	7.08 ± 4.3
	Autumn	11.69 ± 3.14	7.24 ± 2.17	0.29 ± 0.23	3.21 ± 3.28
	Winter	10.68 ± 3.94	6.9 ± 2.28	0.23 ± 0.18	4.61 ± 4.71
<i>L. cajetanus</i>	Agios Stefanos	10.65 ± 2.77	5.18 ± 1.19	0.18 ± 0.09	1.56 ± 2.47
	Plakes	9.6 ± 2.57	4.79 ± 1.16	0.14 ± 0.09	2.72 ± 3.85
	Spring	9.7 ± 2.93	4.78 ± 1.25	0.13 ± 0.07	2.34 ± 3.33
	Summer	10.01 ± 2.88	5.08 ± 1.43	0.16 ± 0.12	2.64 ± 3.09
	Autumn	10.38 ± 2.36	4.98 ± 0.86	0.17 ± 0.08	2.35 ± 3.81
	Winter	10.06 ± 2.43	4.96 ± 0.99	0.14 ± 0.09	2.72 ± 3.85

3.1.1. *Rhyssoplax olivacea*

Rhyssoplax olivacea was the most common species with a sampling size of 2134 specimens. The length–frequency distribution ranged from 1.5 mm to 27 mm in Agios Stefanos and from 2.1 mm to 24.5 mm in Plakes, with modes of 15 mm and 13.5 mm, respectively. Width exhibited values from 1 mm to 16 mm in Agios Stefanos and from 1 mm to 14.5 mm in Plakes, with modes of 9 mm and 8, respectively. Weight exhibited values from 0.001 g to 1.8 g in Agios Stefanos with a mode of 0.45 g and from 0.001 g to 1.5 g in Plakes with a mode of 0.31 g (Table 1, Figure 3). *R. olivacea* exhibits isometry regarding the length–width relationship, while negative allometry was observed for weight–length. Spatial differences were reported for weight–width, which was isometric in Agios Stefanos and negative allometric in Plakes. Spatial comparison between the slopes for the three morphometric relationships indicated that only the length–width slopes were equal (Figure 3).

The results of the two-way ANCOVA indicated that the three morphometric variables are statistically different both spatially and seasonally. Population density followed the same trend with no significant influence from boulder surface (Table 2). The morphometrics of the population of Agios Stefanos exhibited significantly higher values than the population in Plakes. Winter showed the highest values for the three variables while summer and autumn exhibited the lowest values (Table 2). Summer was the only season where the populations did not significantly vary, regarding their morphometrics (Figure 4). Population density increased in spring compared to autumn and was higher in Plakes compared to Agios Stefanos in all seasons, except for autumn, where no significant differences were observed.

Table 2. Two-way ANCOVA and ANOVA results for the effects of region, season, month and surface on the density and morphometric measurements of *R. olivacea*.

Variable	Source of Variation	F	p
Density	Region (Re)	12.07	<0.001
	Season (Se)	3.98	0.01
	Month (M)	1.121	0.35
	Re × M	1.42	0.2
	Re × Se	0.15	0.92
	Surface	0.03	0.84
Length	Region (Re)	69.61	<0.001
	Season (Se)	7.5	<0.001
	Month (M)	3.027	0.001
	Re × M	3.418	<0.001
	Re × Se	4.76	0.002
Width	Region (Re)	68.2	<0.001
	Season (Se)	8.14	<0.001
	Month (M)	2.955	0.001
	Re × M	2.501	0.007
	Re × Se	4.23	0.005
Weight	Region (Re)	107.14	<0.001
	Season (Se)	18.98	<0.001
	Month (M)	8.161	<0.001
	Re × M	5.376	<0.001
	Re × Se	6.77	<0.001

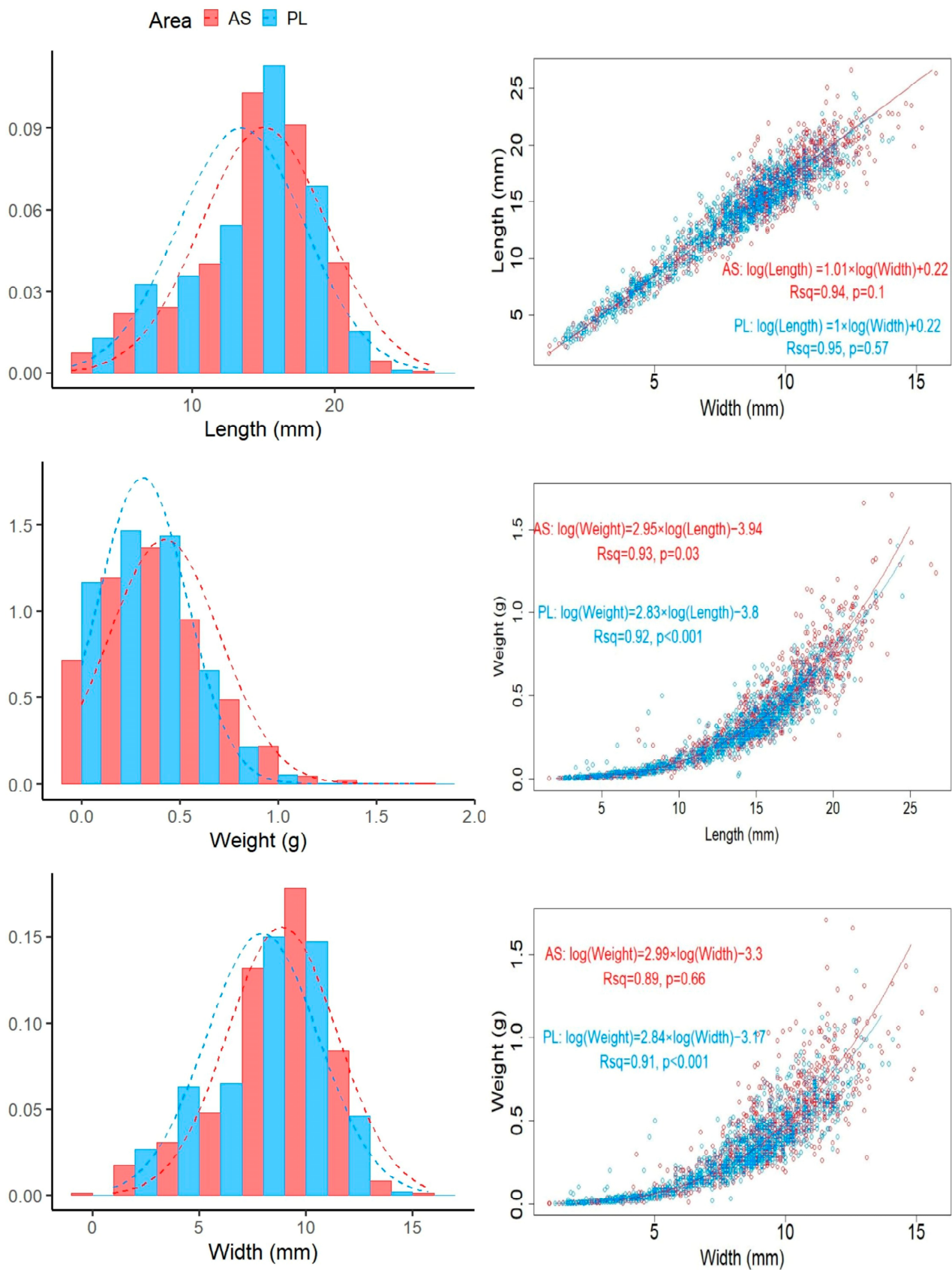


Figure 3. (Top). *R. olivacea* frequency distributions with overlaid fitted normal distribution for Agios Stefanos (AS) and Plakes (PL) for length (mm), weight (g) and width (mm). (Bottom). Morphometric relationships, length/width, weight/width and weight/length of the populations of for the two regions.

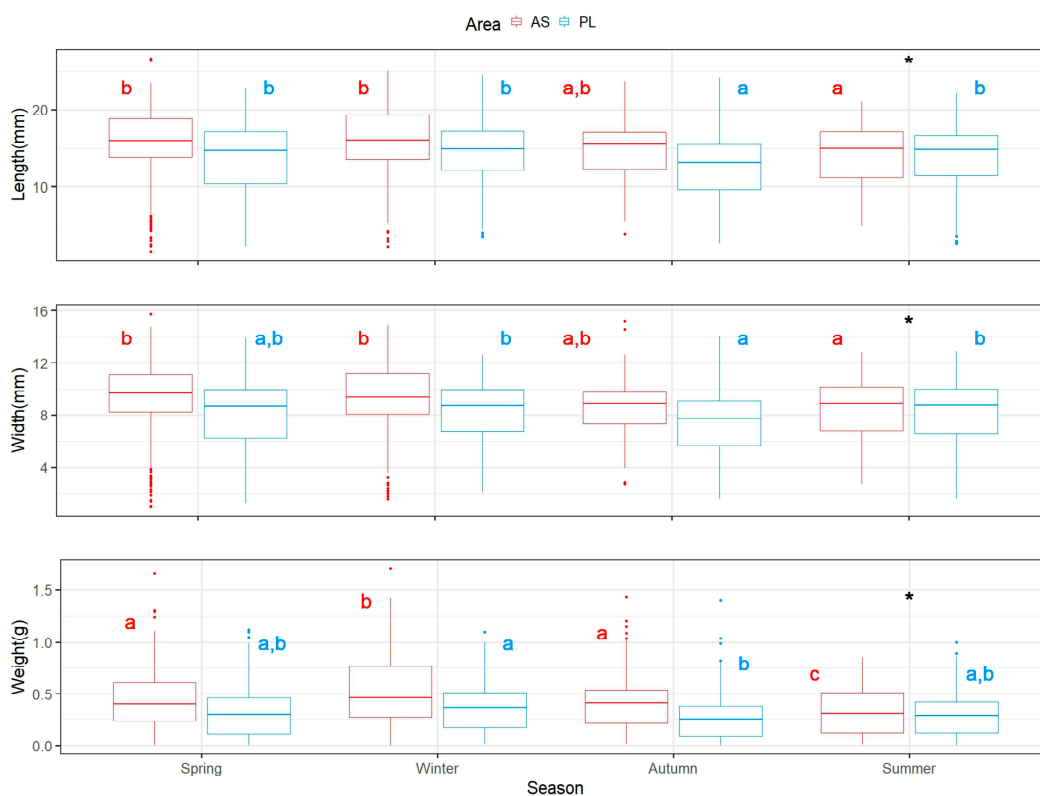


Figure 4. Seasonal variations of morphometric measurements for *R. olivacea* for Agios Stefanos (AS) and for Plakes (PL). Error bars indicate 95% confidence intervals, while centered boxes indicate standard deviation. Different letters indicate significant differences in seasonal morphometrics. Dots indicate outliers, while asterisks (*) denote similarities.

R. olivacea was the only species to report variations for the three morphometric measurements with the effect of month. Spatial variations in length were observed for April, September and February, with Agios Stefanos exhibiting increased length (Figure 5). In Plakes, differences were reported for August with June and July and for September with July, whereas in Agios Stefanos February appears to vary compared to June, July, August, October and April 2023. Regarding width, April and September showed differences between regions, while April significantly varied with June and October in Agios Stefanos, whereas in Plakes August differed from June, July and January, while differences were also observed between September and June (Figure 5). Variations in weight were observed in April and September between the two regions. In Agios Stefanos, February differed with all months except for April, November and April 2023, November varied with April, June, July and October, while March showed significant differences with June and July. In Plakes, weight varied between September and July, December, January, March and April 2023, August with July, December, January and March, April 2023 with August and February, while April varied with January (Figure 5).

3.1.2. *Acanthochitona fascicularis*

Acanthochitona fascicularis was sparser than *R. olivacea*, with 359 specimens recorded. The distributions of the morphometrics showed modes of 12 mm (3–23 mm) and 10.5 mm (2–17.5 mm) for length, 7.5 mm (2–15 mm) and 7 mm (1.5–14 mm) for width and 0.3 g (0.003–1 g) and 0.2 g (0.003–1 g) for weight for Agios Stefanos and Plakes, respectively (Table 1, Figure 6). *A. fascicularis* showed spatial differences for the length–width relationship, with isometry in Agios Stefanos and negative allometry in Plakes. The same trend was observed for weight–width. The relationship between weight and length was isometric for both regions. Slope comparison between the two regions showed significant differences only for the relationship between weight and width (Figure 6).

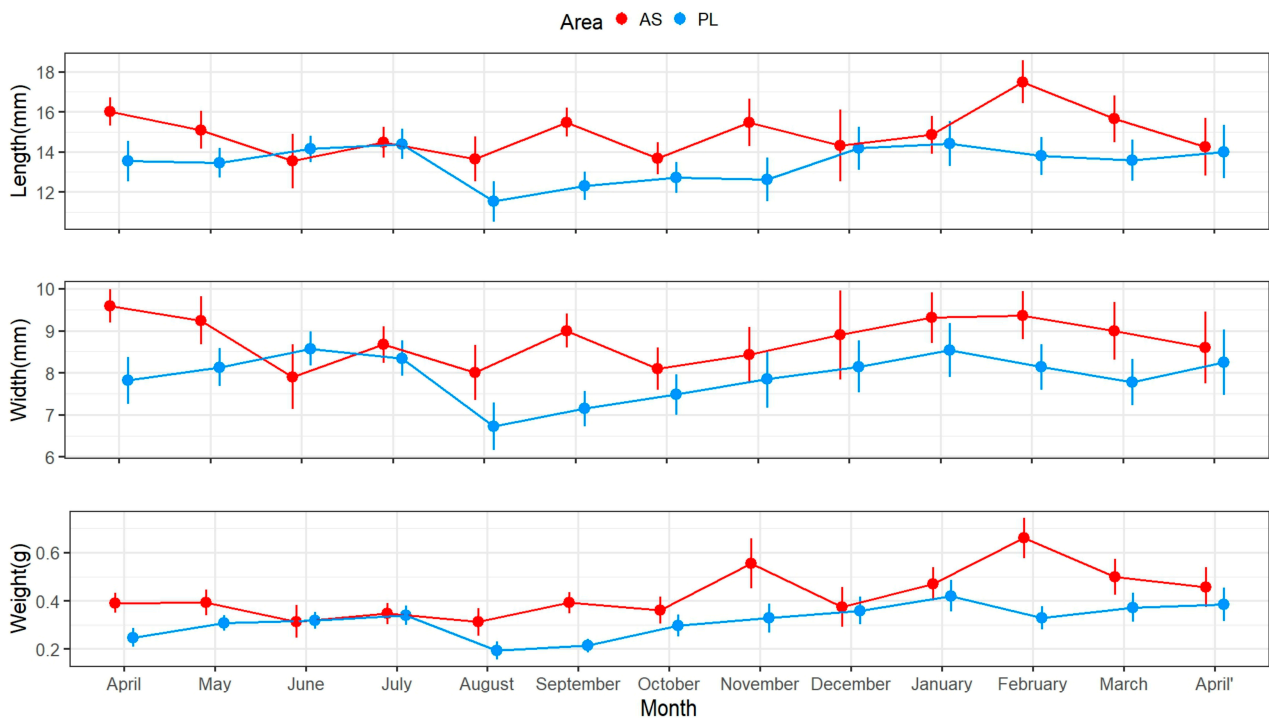


Figure 5. Monthly variations of morphometric measurements for *R. olivacea* for Agios Stefanos (AS) and for Plakes (PL). Error bars indicate 95% confidence intervals, while centered boxes indicate standard deviation.

Both the population density and the morphometrics significantly differed with region; however, only density varied with season (Table 3). The population in Agios Stefanos appears to have higher values compared to Plakes both for the morphometrics and density (Figure 7). The highest density was observed in spring and lowest in autumn, while winter showed no significant differences with summer and autumn. In Agios Stefanos, the weight of *A. fascicularis* in April 2023 showed an increase compared to April 2022, July, August and January.

Table 3. Two-way ANCOVA and ANOVA results for the effects of region, season, month and surface on the density and morphometric measurements of *A. fascicularis*.

Variable	Source of Variation	F	p
Density	Region (Re)	11.13	0.001
	Season (Se)	14.74	<0.001
	Month (M)	0.848	0.56
	Re × M	1.79	0.09
	Re × Se	1.74	0.16
	Surface	2.6	0.1
Length	Region (Re)	18.06	<0.001
	Season (Se)	1.92	0.12
	Month (M)	1.191	0.3
	Re × M	0.732	0.67
	Re × Se	2.66	0.04
Width	Region (Re)	11.18	<0.001
	Season (Se)	0.5	0.65
	Month (M)	0.772	0.652
	Re × M	0.617	0.782
	Re × Se	1.35	0.25
Weight	Region (Re)	8.876	0.003
	Season (Se)	0.61	0.6
	Month (M)	2.848	0.003
	Re × M	1.233	0.273
	Re × Se	2.48	0.06

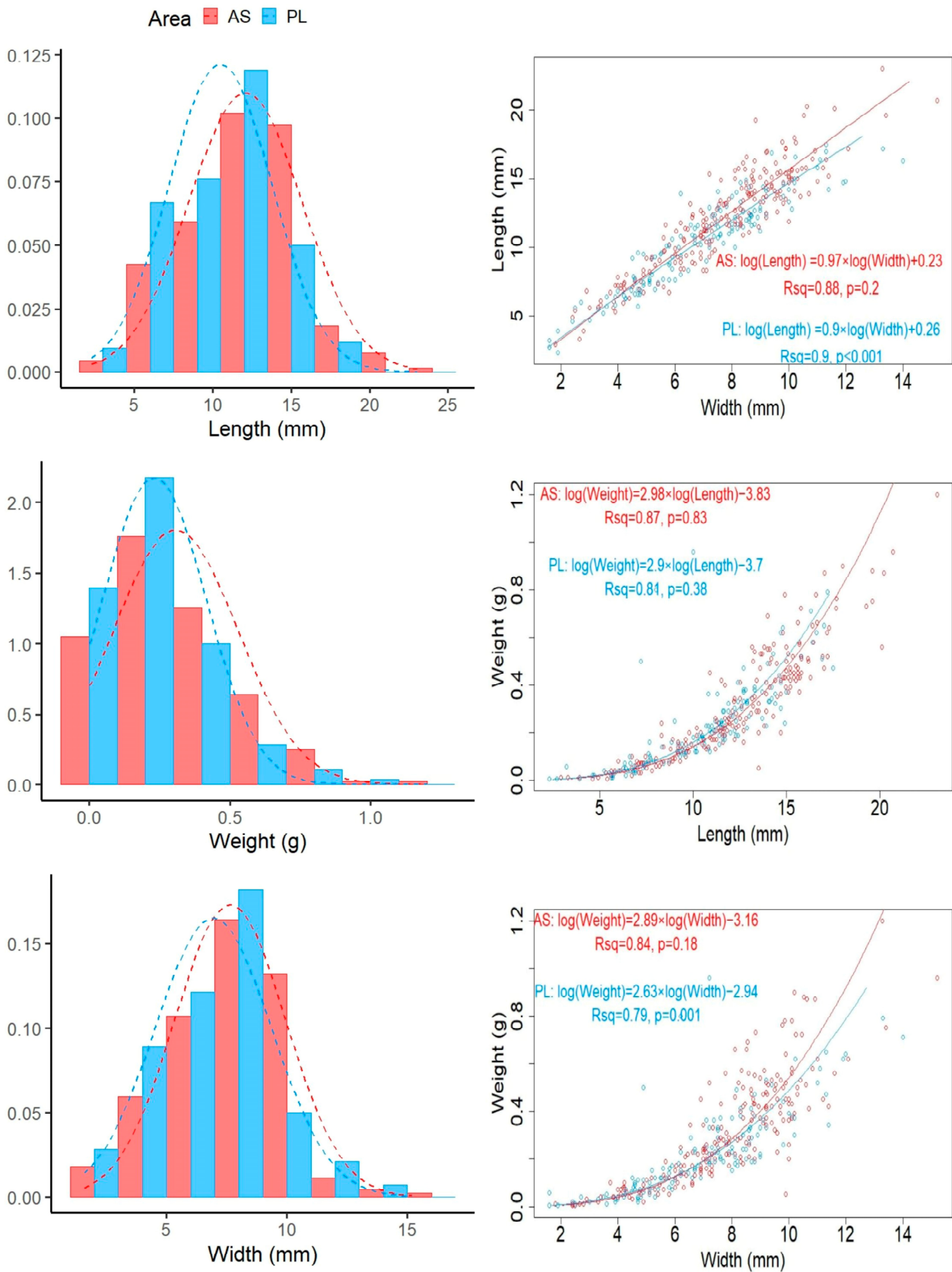


Figure 6. (Top). *A. fascicularis* frequency distributions with overlaid fitted normal distribution for Agios Stefanos (AS) and Plakes (PL) for length (mm), weight (g) and width (mm). **(Bottom).** Morphometric relationships, length/width, weight/width and weight/length of the populations of *A. fascicularis* for the two regions.

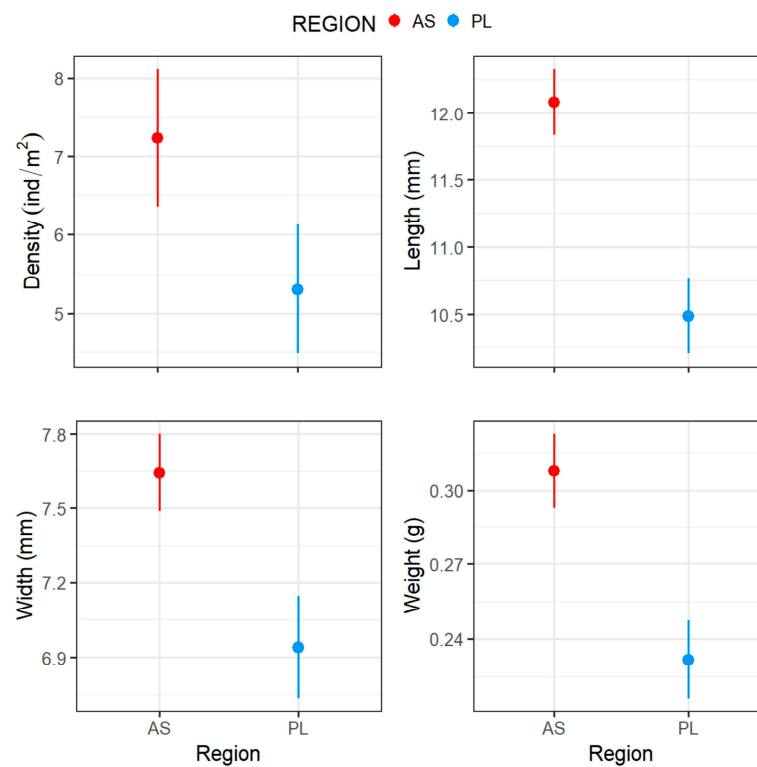


Figure 7. Regional variations of morphometric measurements and population density for *A. fascicularis* for Agios Stefanos (AS) and for Plakes (PL). Error bars indicate 95% confidence intervals, while centered boxes indicate standard deviation.

3.1.3. *Lepidopleurus cajetanus*

Lepidopleurus cajetanus was the rarest out of the three species, with 121 individuals sampled. The morphometric distributions for Agios Stefanos ranged from 2.5 mm to 14.5 mm with a mode of 10.5 mm for length, from 1 mm to 7 mm for width with a mode of 5 mm and from 0.005 g to 0.4 g for weight with a mode of 0.2 g. In Plakes, the length presented a mode of 9.5 mm (2.5–18 mm), width of 5 mm (1.5–11 mm) and weight of 0.15 (0.004–0.7 g), (Table 1, Figure 8). The length–width and weight–width relationships showed isometry for Agios Stefanos and positive allometric in Plakes, whereas weight–length was reported to be negative allometric for both regions. Slope comparison determined that only the slopes for weight–length did not differ with region (Figure 8).

The population of Agios Stefanos exhibited significantly higher morphometric values, while increased density was observed in Plakes (Figure 9). None of the studied parameters appeared to vary in any examined temporal resolution; however, boulder surface seems to affect the population density of this species (Table 4).

3.2. Dispersion Pattern

The populations of all species deviated from a Poisson distribution (chi-squared test) and exhibited a clumped distribution (standardized Morisita index > 0.5), with the exception of the *A. fascicularis* population in Plakes in autumn and winter, where both the chi-squared test and *inst* indicated a random distribution (Table 5).

3.3. Growth Parameters

The growth curves for the three examined species are superimposed on restructured LFQ data, with black and white bars and a blue and red background corresponding to positive and negative deviations from the moving average, respectively (Figure 10). Best fit estimates with lower and upper margins for 95% confidence intervals for the resulting growth parameters are presented in Tables 5–7 for *R. olivacea*, *A. fascicularis* and *L. cajetanus*, respectively.

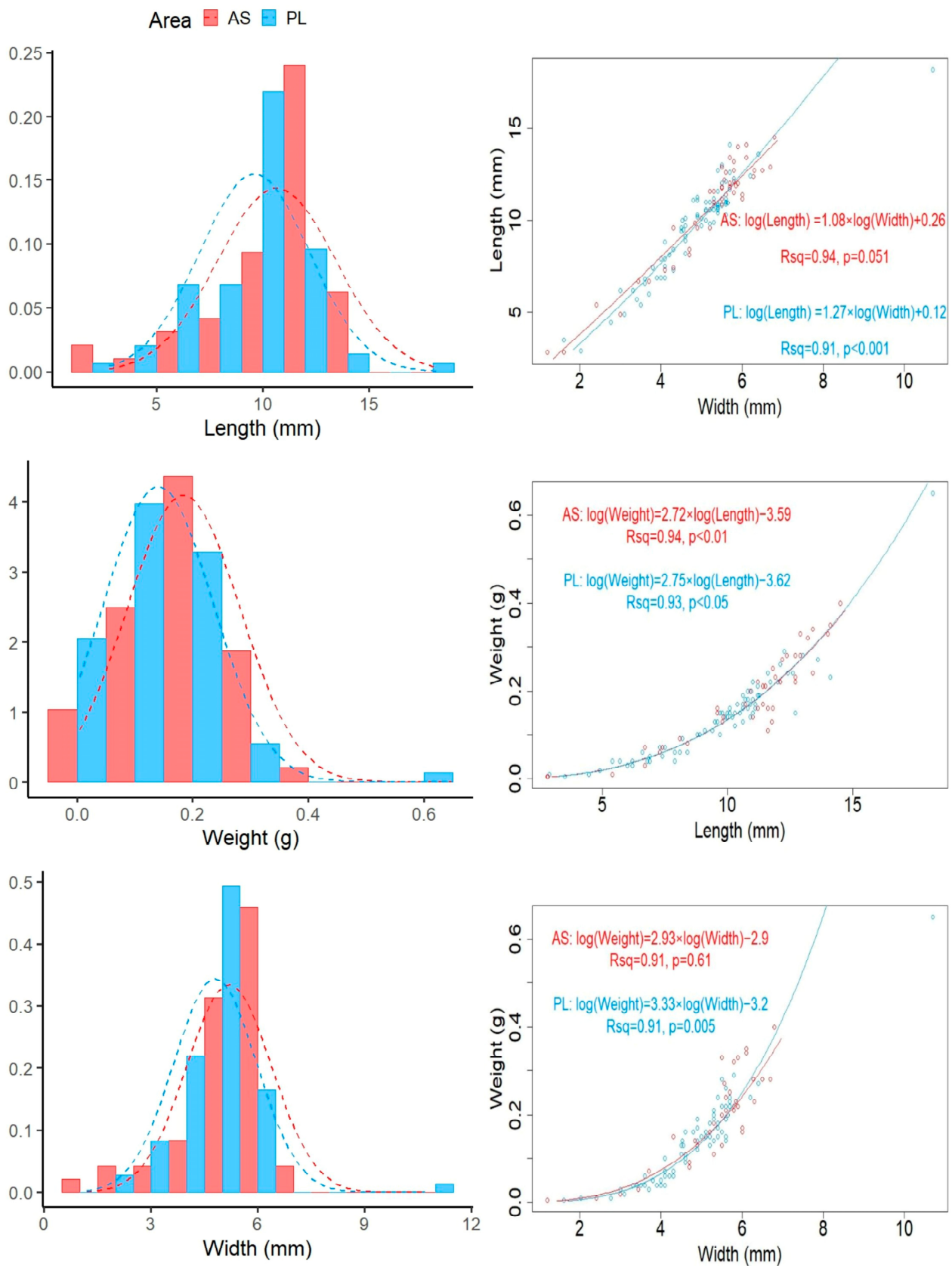


Figure 8. (Top). *L. cajetanus* frequency distributions with overlaid fitted normal distribution for Agios Stefanos (AS) and Plakes (PL) for length (mm), weight (g) and width (mm). **(Bottom).** Morphometric relationships, length/width, weight/width and weight/length of the populations of *L. cajetanus* for the two regions.

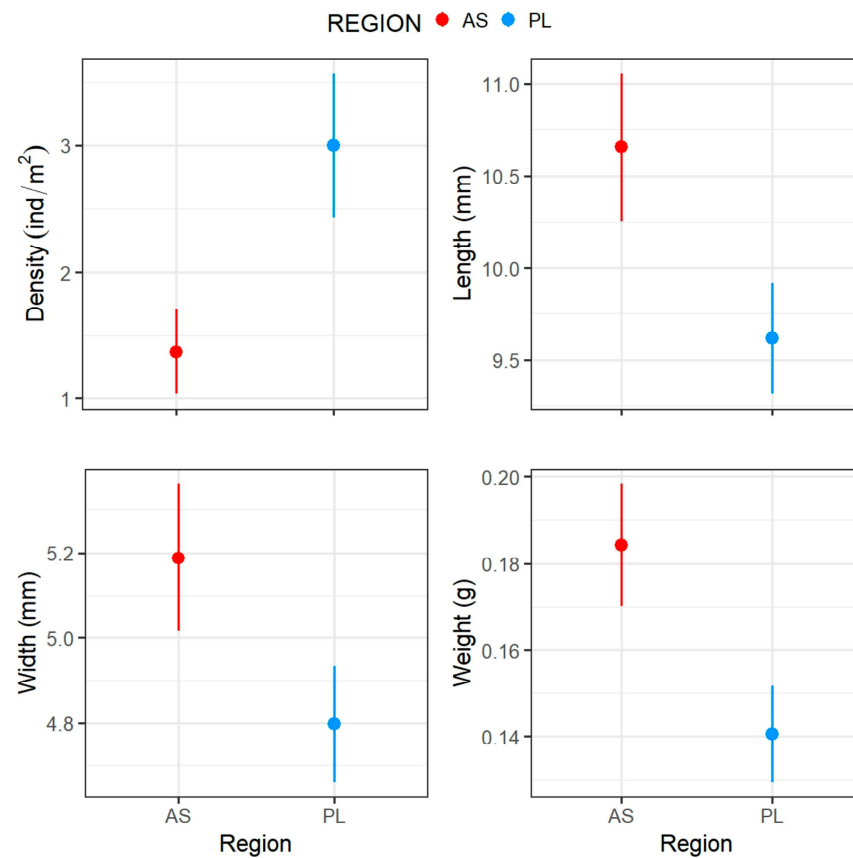


Figure 9. Regional variations of morphometric measurements and population density for *L. cajetanus* for Agios Stefanos (AS) and Plakes (PL). Error bars indicate 95% confidence intervals, while centered boxes indicate standard deviation.

Table 4. Two-way ANCOVA and ANOVA results for the effects of region, season, month and surface on the density and morphometric measurements of *L. cajetanus*.

Variable	Source of Variation	F	p
Density	Region (Re)	4.78	0.03
	Season (Se)	0.97	0.4
	Month (M)	1.525	0.16
	Re × M	1.36	0.22
	Re × Se	2.94	0.03
	Surface	5.84	0.01
	Length	Region (Re)	6.954
Season (Se)		0.54	0.65
Month (M)		1.65	0.11
Re × M		0.638	0.723
Re × Se		0.79	0.5
Width		Region (Re)	6.329
	Season (Se)	0.259	0.85
	Month (M)	1.83	0.07
	Re × M	0.504	0.829
	Re × Se	0.9	0.44
	Weight	Region (Re)	11.752
Season (Se)		1.45	0.23
Month (M)		0.88	0.53
Re × M		0.639	0.72
Re × Se		1.16	0.32

Table 5. Dispersion pattern of *R. olivacea*, *A. fascicularis* and *L. cajetanus* at each sampling site and season. *imst*, standardized Morisita index of dispersion value; *p*, chi-square test value for each distribution. *p* values in bold indicate statistical significance ($p < 0.05$).

Region	Season	<i>R. olivacea</i>		<i>A. fascicularis</i>		<i>L. cajetanus</i>	
		<i>Imst</i>	<i>p</i>	<i>Imst</i>	<i>p</i>	<i>Imst</i>	<i>p</i>
AGIOS STEFANOS	Spring	0.512	<0.001	0.508	<0.001	0.519	0.005
	Summer	0.515	<0.001	0.501	0.01	0.526	<0.001
	Autumn	0.502	<0.001	0.531	<0.001	0.549	0.002
	Winter	0.509	<0.001	0.528	<0.001	0.812	<0.001
PLAKES	Spring	0.501	<0.001	0.507	<0.001	0.654	<0.001
	Summer	0.503	<0.001	0.511	<0.001	0.565	<0.001
	Autumn	0.505	<0.001	0.149	0.21	0.528	<0.001
	Winter	0.506	<0.001	−0.238	0.73	0.549	0.002

Table 6. Parameter estimates of the seasonally oscillating VBGF for *R. olivacea*. Estimated by a bootstrapped ELEFAN_GA. Lower and upper denoted 95% confidence interval margins.

Species	Parameter	Mod	Lower	Upper
<i>R. olivacea</i>	<i>Linf</i> (mm)	19.89	18.13	41.5
	<i>K</i> (y^{-1})	0.77	0.29	0.89
	<i>t_{anchor}</i>	0.69	0.59	0.83
	<i>C</i>	0.46	0.16	0.88
	<i>T_s</i>	0.66	0.35	0.88
	Φ	2.45	2.38	2.65
	<i>Longevity</i>	4.72		

Table 7. Parameter estimates of the seasonally oscillating VBGF for *A. fascicularis*. Estimated by a bootstrapped ELEFAN_GA. Lower and upper denoted 95% confidence interval margins.

Species	Parameter	Mod	Lower	Upper
<i>A. fascicularis</i>	<i>Linf</i> (mm)	26.56	23.24	32.84
	<i>K</i> (y^{-1})	0.7	0.44	0.93
	<i>t_{anchor}</i>	0.28	0.01	0.97
	<i>C</i>	0.48	0.27	0.84
	<i>T_s</i>	0.64	0.34	0.95
	Φ	2.74	2.22	2.85
	<i>Longevity</i>	3.47		

3.3.1. *Rhysoplax olivacea*

The optimization routine for the bootstrapped ELEFAN_GA that was used to estimate the L_{∞} and *K* values that best fit the VBGF curves tended to become trapped in a small range of local maxima for both parameters, while a second group of L_{∞} and *K* values could be observed, although with a substantially smaller number of observations (Figure 10). The optimum value for *t_{anchor}* suggests that the time at which length equals zero is approximately on the 12th of September. The seasonally oscillating index *C* indicates a relatively strong growth oscillation, with *t_s* exhibiting a positive turn in growth in August, where sine wave oscillations begin (*t_s* = 0.5 means positive turn in growth on 1st July) [24].

Using the VBGF equation, length = $19.89 \times (1 - e^{-0.77 \times (\text{Age} + 0.108913)})$; the length–age curve was constructed (Figure 11). The growth performance index was similar to those of the other species (Table 6). The linear growth equation describing the pooled population of *R. olivacea* was estimated as length = 4.7*age + 4.48, while longevity was approximately 4.7 years.

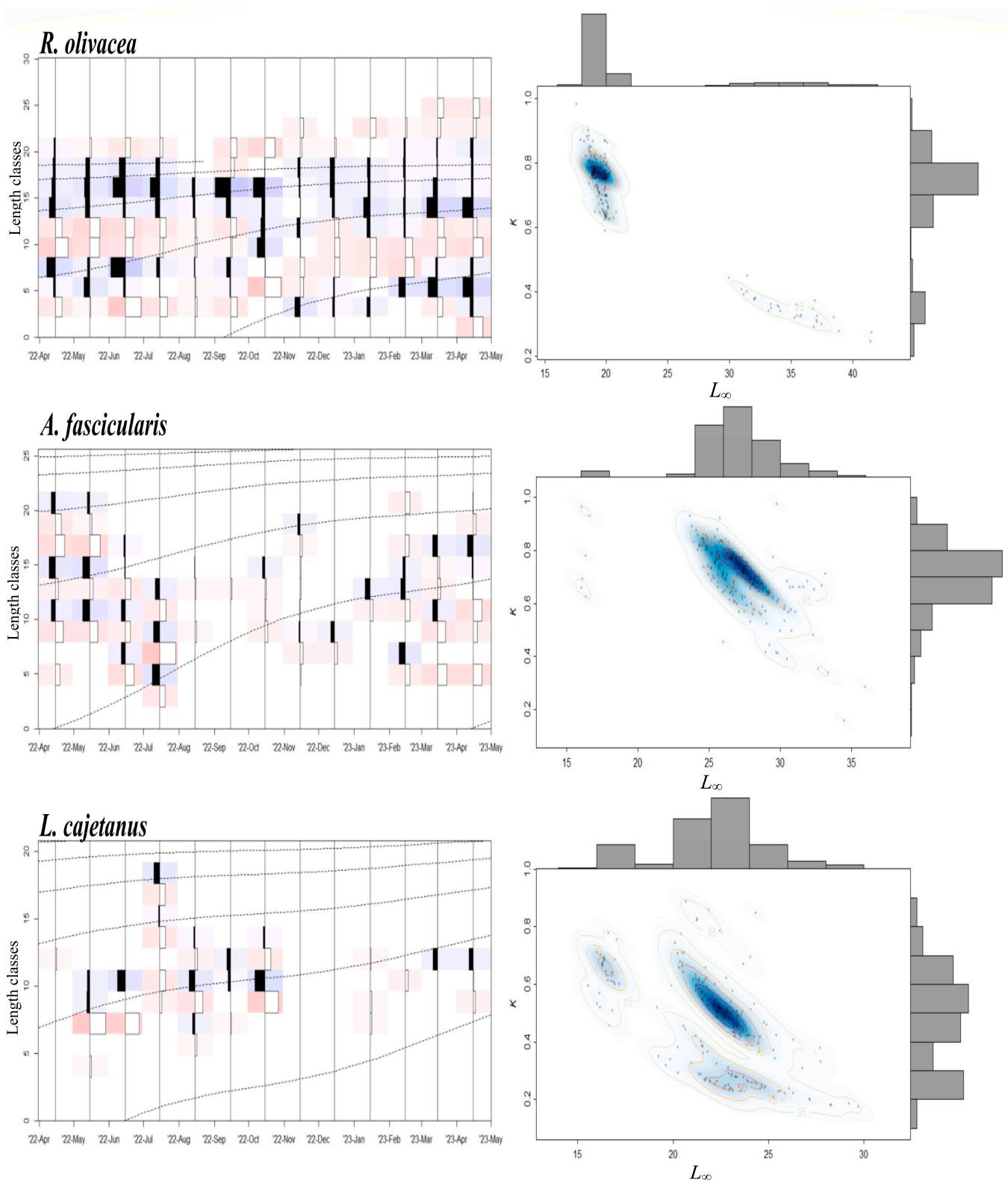


Figure 10. (Left). Length frequency data and growth curves from restructure data (*R. olivacea*: MA = 5, *A. fascicularis* and *L. cajetanus* MA = 3), obtained through the seasonally oscillating bootstrapped ELEFAN_GA. Bars represent restructured length frequency data, with black–white bars and blue–red background indicating positive and negative picks, respectively. **(Right).** Scatter histogram of bootstrapped ELEFAN_GA for the three species. Each point represents a simple combination of L_∞ and K , while the densities of the combinations are depicted as contours. Histograms represent marginal distributions of L_∞ and K .

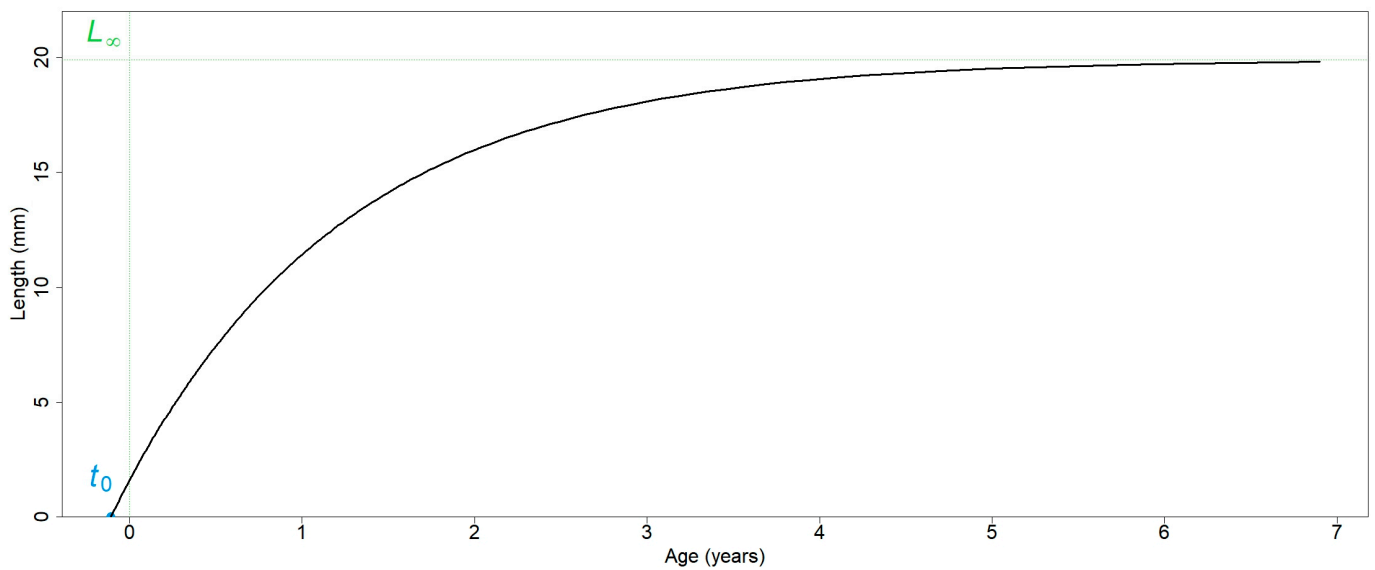


Figure 11. Growth curve of *R. olivacea* constructed using the optimum growth parameters from the bootstrapped ELEFAN_GA. Asymptotic length (L_∞) and time at which length equals zero (t_0) are annotated.

3.3.2. *Acanthochitona fascicularis*

Bootstrapped ELEFAN_GA estimations for the L_∞ and K values for this species appear to be constricted around 23.24–32.84 mm and $0.44\text{--}0.93\text{ y}^{-1}$, respectively. The time corresponding to zero length is expected in mid-April, as suggested by t_{anchor} (Figure 10). The strength of growth oscillation was similar to that of the other two species, while a positive turn in growth is observed in August (Table 7).

From the equation, $\text{length} = 26.56 \times (1 - e^{-0.7 \times (\text{Age} + 0.129396)})$, the length–age curve was constructed (Figure 12). The linear growth equation for *A. fascicularis* is $\text{Length} = 4.19 \times \text{Age} + 8.44$, with a maximum lifespan of 3.47 years.

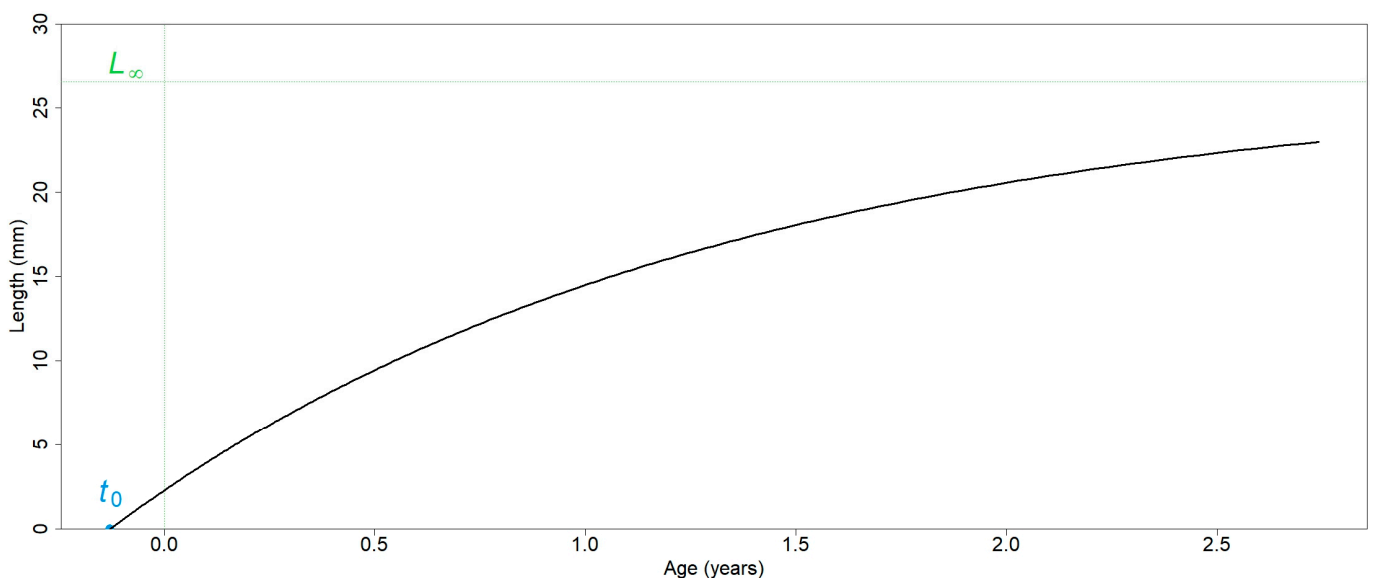


Figure 12. Growth curve of *A. fascicularis* constructed using the optimum growth parameters from the bootstrapped ELEFAN_GA. Asymptotic length (L_∞) and time at which length equals zero (t_0) are annotated.

3.3.3. *Lepidopleurus cajetanus*

The bootstrapped ELEFAN_GA method exhibits a single group of values for L_∞ but a relatively increased variation regarding the K values (Figure 10). This species presents lower K values compared to the other two, coupled with higher longevity (Table 8). Sine wave oscillations begin in May.

Table 8. Parameter estimates of the seasonally oscillating VBGF for *L. cajetanus*. Estimated by a bootstrapped ELEFAN_GA. Lower and upper denoted 95% confidence interval margins.

Species	Parameter	Mod	Lower	Upper
<i>L. cajetanus</i>	L_{inf} (mm)	22.85	15.43	26.74
	K (y^{-1})	0.5	0.18	0.73
	T_{anchor}	0.45	0.1	0.68
	C	0.51	0.18	0.97
	T_s	0.25	0.12	0.95
	Φ	2.42	2.07	2.5
	Longevity	3.41		

The von Bertalanffy growth equation for this species was estimated as: length = $22.85 \times (1 - e^{-0.5 \times (\text{Age} + 0.261444)})$, (Figure 13). The linear relationship between length at age of *L. cajetanus* is described by the equation: length = $3.53 \times \text{age} + 5.98$, while the maximum lifespan for this species is estimated to be 3.41 years.

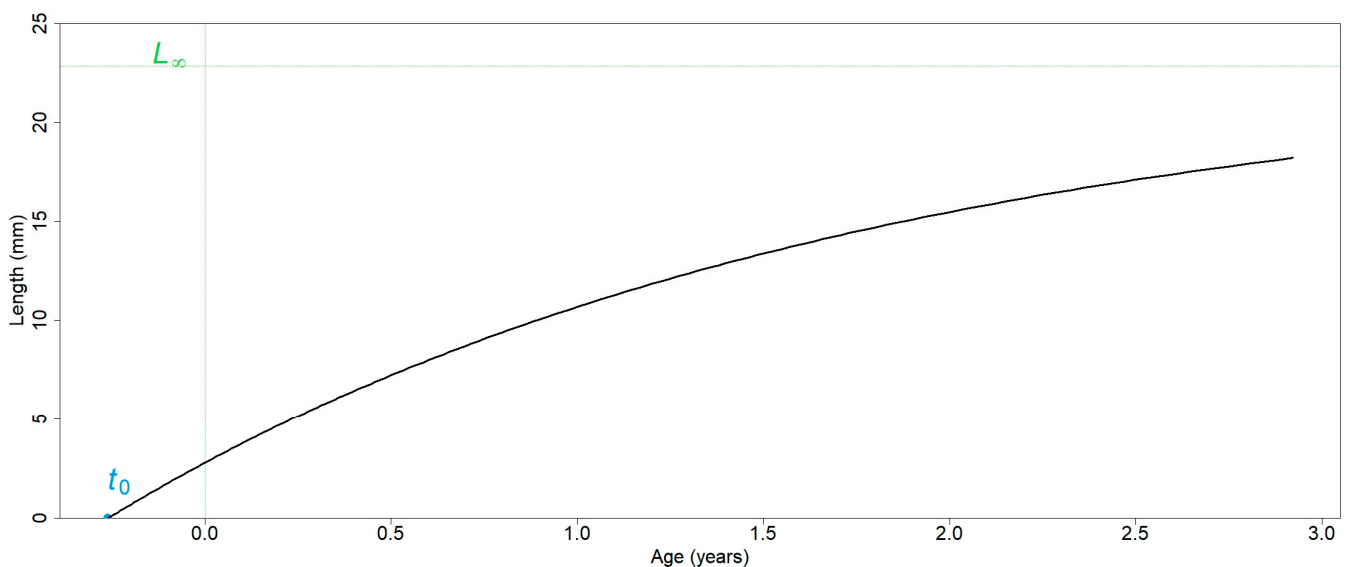


Figure 13. Growth curve of *L. cajetanus* constructed using the optimum growth parameters from the bootstrapped ELEFAN_GA. Asymptotic length (L_∞) and time at which length equals zero (t_0) are annotated.

4. Discussion

Previous studies in the eastern Mediterranean focused on the presence and species composition of Polyplacophora, rather than spatio-temporal changes in specific populations. *Rhyssoplax olivacea* was characterized as the dominant chiton species in the eastern coasts of Turkey and the most common in Greece, as also shown in the present study [32,33]. This species was the only one to exhibit both spatial and temporal differences in population density and individual size. Region was the main factor affecting the densities and sizes for all species. The present study examined the temporal effect in two scales (season, month) and reported a different influence for each species. Monthly changes in weight may result from a series of reproductive processes taking place throughout the year, as shown by previous

literature [21,34]. If this is the case for the species examined here, then the present results might infer some variation in reproductive strategies, although further research is necessary.

The relationship between the size of boulder and the number of individuals has been previously tested for species of the genus *Ischnochiton* in Australia, where no significance was found [12]. In the present study, *Lepidopleurus cajetanus* was the only species where a relationship between boulder surface and density was reported (Table 4). However, the underlying causes as to why this species shows a preference for larger boulders is yet unclear. This species is reported to be mostly found under stones embedded in sand, the underside colors of these stones matching the yellow or whitish color of the animals [32]. This has also been observed for a number of other species; for instance, the red colored chiton *Callochiton septemvalvis* on red algae, the white *Stenosemus albus* on white algae, while color morphs for *Lepidochitona cinerea* and *Acanthochitona crinita* were found in habitats with matching colors [35,36]. During field sampling, this tendency was also observed for *L. cajetanus* in the present study (authors' observations). The preference in boulder size combined with the hypothesized camouflage behavior might serve as a defensive mechanism against both predators and disturbance, since smaller boulders are more easily overturned through wave action.

Generally, chitons are characterized by a more-or-less oval body shape, which, however, can vary from broad oval to vermiform among the 1000 living species [37]. Intra- and interspecific allometric shifts in body shape and size are sometimes related to a particular niche adaptation [38]. Allometry in chitons is also closely related to life stage, as was shown in previous studies [21]. Data on polyplacophoran allometry are mainly available for tropical environments, where both negative and positive allometries have been observed for different species (see [18] for more details). For *Chiton articulatus*, a latitudinal shift in weight–length has been observed, with increased b values reported with increased latitude, which might be explained by the ectothermic nature of this species [19]. In the present study, several differences were observed regarding the allometric relationships among the examined morphometric variables for all species with the effect of region. Since the two sites are in close proximity with each other, intraspecific differences might be explained by other environmental or biotic factors, potentially resulting in some physiological variations. More importantly, the three species exhibited different allometric trends, with *Acanthochitona fascicularis* showing isometry for the weight–length relationship (Figure 6), while *L. cajetanus* was the only species where positive allometry was reported (Figure 8). Differences in allometry often result from environmental and habitat adaptations, while they might also infer changes in resource and energy allocation during different ontogenetic or reproductive stages ([18,20,21,38–40]). This might indicate differences in terms of environmental influence and habitat adaptations, possibly leading to different ecological niche occupation among the three species. Future studies examining the shift in allometric trends for different life stages or for different reproductive periods will help in explaining the inter- and intraspecific differences in allometry observed here.

Mollusks on intertidal boulder fields often show aggregated patterns of dispersion [40]. Many factors have been proposed to result in clustered patterns, some of those being stress as a result of desiccation, wave action or food availability [41–43]. However, a study on the genus of *Ischnochiton* in southern Australia concluded that physical stress did not influence the dispersion of these species. Furthermore, the same study reported no clear relationships between the dispersion of chitons and other assemblages neither on nor under boulders [12]. In the present study, the three examined species exhibited spatio-temporal aggregated patterns, except for *A. fascicularis* in autumn and winter. *L. cajetanus* exhibited the highest overdispersion with spatio-temporal fluctuations, whereas the overdispersion pattern of *R. olivacea* seems to remain constant.

Published data regarding mostly large chitons from tropical waters hypothesize that these organisms are relatively long-lived, while exhibiting slow growth [44–46]. For *Katharina tunicata*, the growth parameters L_{∞} and K were estimated to be 114 mm and 0.217, with an observed maximum age 17 years. An examination of the growth of *Plaxiphora aurata* in

Argentina reported values of 53 mm and 0.359 for L_{∞} and K , respectively, while longevity was estimated at 6–7 years [15]. For *Chiton articulatus* in Mexico, L_{∞} was estimated at 71.5 and 81 mm for cold and warm annual events, respectively, using Schnute models. The same study reported maximum ages of 2.6 and 1.3 years, although these results would correspond to 5.2 and 4.7 years if the von Bertalanffy equation was used [17]. However, one study on *Acanthochitona rectrojecta*, a small-sized chiton, indicated differences in the reproduction, growth and mortality of this species compared to other larger, co-occurring chitons [9]. For *Acanthochitona crinite*, lifespan was estimated at nearly 1 year [47].

In the present study, the estimated values for L_{∞} were substantially lower, while K values appeared to be two to three times higher. Longevity ranged from 4.72 years for *R. olivacea* to 3.4 years for *L. cajetanus* and *A. fascicularis*. These values for maximum age are similar with those reported for larger species in tropical environments. However, the present study might overestimate the longevity of the three species, due to limitations regarding the growth estimates induced by potential constant recruitment. A seasonal variation in growth rates is often reported for various species, predominately a decrease in winter and increase during spring and summer [15,48,49]. Using the seasonal oscillation index and t_s , the present study reports a strong positive term in growth during spring for *L. cajetanus* and during August for *R. olivacea* and *A. fascicularis*. Recently, it was found that *L. cajetanus* might represent a complex of species occurring throughout the Mediterranean, rather than a single species [50]. This might introduce additional variation regarding the growth parameters presented here.

This is the first study to report spatial and temporal variations in shape and size regarding three co-occurring shallow sublittoral Polyplacophora species from the Eastern Mediterranean Sea. Although overdispersion was observed for all species, the reasons leading to clustered aggregations for these organisms are yet largely unknown. The three species exhibited different allometric patterns, possibly due to differences in a combination of ecological adaptations (e.g., resistance to disturbance) and reproductive strategies (e.g., recruitment patterns), which might be related to differences in resource allocation. Finally, it is the first time that specific parameters for growth and age are reported for chitons native to the Mediterranean Sea. The ecological aspects of the Mediterranean Polyplacophora are largely understudied, leading to a gap in knowledge regarding the ecological zones, especially the shallow sublittoral, where they are most commonly found. Further research towards their interactions with other organisms, as well as their reproduction, needs to be conducted, especially regarding their ecological niches and potential competition for food or space.

Author Contributions: Conceptualization A.V., K.V. and D.V.; methodology A.V., K.V. and D.S.Z.; formal analysis A.V., K.V. and D.V.; project administration D.V.; supervision D.V.; visualization A.V., K.V. and D.V.; writing—original draft A.V. and K.V.; writing—review and editing A.V., K.V. and D.V. All authors have read and agreed to the published version of the manuscript.

Funding: This research received no external funding.

Data Availability Statement: The datasets generated and analyzed during the current study are available from the author on reasonable request.

Acknowledgments: The authors would like to thank the undergraduate student Thomas Migdalias for his assistance during the field samplings.

Conflicts of Interest: The authors declare no conflict of interest.

References

1. Kaas, P.; Van Belle, R.A.; Strack, H.L. Monograph of living chitons. (Mollusca: Polyplacophora)6, Suborder Ischnochitonina (concluded): Schizochitonidae; Chitonidae. In *Additions to Volumes*; Koninklijke Brill NV: Leiden, The Netherlands, 2006; Volume 463, pp. 1–5.
2. Elahi, R.; Sebens, K. Consumers mediate natural variation between prey richness and resource use in a benthic marine community. *Mar. Ecol. Prog. Ser.* **2012**, *452*, 131–143. [[CrossRef](#)]

3. Barbosa, S.S.; Byrn, M.; Kelaher, B.P. Bioerosion caused by foraging of the tropical chiton *Acanthopleura gemmata* at One Tree Reef, southern Great Barrier Reef. *Coral Reefs* **2008**, *27*, 635–639. [[CrossRef](#)]
4. Vafidis, D.; Drosou, I.; Dimitriou, K.; Klaoudatos, D. Population Characteristics of the Limpet *Patella caerulea* (Linnaeus, 1758) in Eastern Mediterranean (Central Greece). *Water* **2020**, *12*, 1186. [[CrossRef](#)]
5. Klaoudatos, D.; Kotsiri, Z.; Neofitou, N.; Lolas, A.; Vafidis, D. Population Characteristics of the Mid-Littoral Chthamaliid Barnacle *C. stellatus* (Poli, 1791) in Eastern Mediterranean (Central Greece). *Water* **2020**, *12*, 3304. [[CrossRef](#)]
6. Koukouras, A.; Karachle, P. The Polyplacophoran (Eumollusca, Mollusca) fauna of the Aegean Sea with the description of a new species, and comparison with those of neighbouring areas. *J. Biol. Res.* **2005**, *3*, 23–38.
7. Dell'Angelo, B.; Smriglio, C. *Living Chitons of the Mediterranean*; Edizioni Evolver: Rome, Italy, 2001.
8. Olabarria, C.; Chapman, M.G. Comparison of patterns of spatial variation of microgastropods between 2 contrasting intertidal habitats. *Mar. Ecol. Prog. Ser.* **2001**, *220*, 201–211. [[CrossRef](#)]
9. Kelaher, B.P.; Cole, V. Variation in abundance and size-structure of populations of the small chiton, *Acanthochitona Retrojecta*. *J. Molluscan Stud.* **2005**, *71*, 145–151. [[CrossRef](#)]
10. Underwood, A.J. *Experiments in Ecology: Their Logical Design and Interpretation Using Analysis of Variance*; Cambridge University Press: Cambridge, MA, USA, 1997; Volume 2, p. 504.
11. Smith, K.A.; Otway, N.M. Spatial and temporal patterns of abundance and effects of disturbance on under-boulder chitons. *Molluscan Res.* **1997**, *18*, 43–57. [[CrossRef](#)]
12. Grayson, J.; Chapman, M.G. Patterns of distribution and abundance of chitons of the genus *Ischnochiton* in intertidal boulder fields. *Austral Ecol.* **2004**, *29*, 363–373. [[CrossRef](#)]
13. Otway, N.M. Population ecology of the low-shore chitons *Onithochiton querinus* and *Plaxiphora albida*. *Mar. Biol.* **1994**, *121*, 105–116. [[CrossRef](#)]
14. Lord, J.P.; Shanks, A.L. Continuous growth facilitates feeding and reproduction: Impact of size on energy allocation patterns for organisms with indeterminate growth. *Mar. Biol.* **2012**, *159*, 1417–1428. [[CrossRef](#)]
15. López-Gappa, J.; Tablado, A. Growth and Production of an Intertidal Population of the Chiton *Plaxiphora aurata* (Spalowski, 1795). *Veliger* **1997**, *40*, 263–270.
16. Begg, G.A. Chapter 6—Life history parameters. In *Stock Identification Methods—Applications in Fishery Science*; Cadrin, S.X., Friedland, K.D., Cadrin, S.X., Friedland, K.D., Waldman, J.R., Eds.; Elsevier Academic Press: Burlington, MA, USA, 2005; pp. 119–150.
17. Avila-Poveda, O.H.; Rodriguez-Dominguez, G.; Ramirez-Perez, J.S.; Perez-Gonzalez, R. Plasticity in Growth Parameters of an Intertidal Rocky Shore Chiton (Polyplacophora: Chitonida) under Pre-ENSO and ENSO Events. *J. Molluscan Stud.* **2019**, *86*, 72–78. [[CrossRef](#)]
18. Valencia-Cayetano, C.; García-Ibáñez, S.; Avila-Poveda, O.H.; Padilla-Serrato, J.G.; Violante-González, J.; Flores-Garza, R. Using a fisherman's harvest in Acapulco, México, to characterize population structure, allometry, and body condition in the edible intertidal mollusc *Chiton articulatus* (Chitonida: Chitonidae). *Reg. Stud. Mar. Sci.* **2023**, *62*, 2352–4855. [[CrossRef](#)]
19. Guillen, C.; Marquez-Farias, J.F.; Avila-Poveda, O.H. Body size variation in an intertidal polyplacophora along a tropical latitudinal gradient. In Proceedings of the 9th European Congress of Malacological Societies Euromal, Online, 5–9 September 2021.
20. Ibáñez, C.M.; Sepúlveda, R.D.; Sigwart, J.D. Comparative allometric variation in intertidal chitons (Polyplacophora: Chitonidae). *Zoomorphology* **2018**, *137*, 249–256. [[CrossRef](#)]
21. Avila-Poveda, O.H.; Abadia-Chanona, Q.Y. Emergence, development, and maturity of the gonad of two species of chitons “sea cockroach” (Mollusca: Polyplacophora) through the early life stages. *PLoS ONE* **2013**, *8*, e69785. [[CrossRef](#)]
22. Schneider, C.A.; Rasband, W.S.; Eliceiri, K.W. NIH Image to ImageJ: 25 years of image analysis. *Nat. Methods* **2012**, *9*, 671–675. [[CrossRef](#)]
23. Warton, D.I.; Duursma, R.A.; Falster, D.S.; Taskinen, S. Smatr 3—An R package for estimation and inference about allometric lines. *Methods Ecol. Evol.* **2012**, *3*, 257–259. [[CrossRef](#)]
24. Smith-Gill, S.J. Cytophysiological basis of disruptive pigmentary patterns in the leopard frog, *Rana pipiens*. II. Wild type and mutant cell specific patterns. *J. Morphol.* **1975**, *146*, 35–54. [[CrossRef](#)] [[PubMed](#)]
25. Mildenerger, T.K.; Taylor, M.H.; Wolff, M. TropFishR: An R package for fisheries analysis with length-frequency data. *Methods Ecol. Evol.* **2017**, *8*, 1520–1527. [[CrossRef](#)]
26. Pauly, D. On the Interrelations between Natural Mortality, Growth Parameters and Mean Environmental Temperature in 175 Fish Stocks. *ICES J. Mar. Sci.* **1980**, *39*, 175–192. [[CrossRef](#)]
27. Schwamborn, R.; Mildenerger, T.K.; Taylor, M.H. Assessing sources of uncertainty in length-based estimates of body growth in populations of fishes and macroinvertebrates with bootstrapped ELEFAN. *Ecol. Model.* **2019**, *393*, 37–45. [[CrossRef](#)]
28. Wang, B.; Fan, S.; Pan, J.; Ting, X.; Zhenlong, F.; Quan, W. Research on predicting the productivity of cutter suction dredgers based on data mining with model stacked generalization. *Ocean Eng.* **2020**, *217*, 108001. [[CrossRef](#)]
29. Pauly, D.; Munro, J.L. Once more on growth comparisons in fish and invertebrates. *Fishbyte* **1984**, *2*, 21.
30. Ba, K.; Thiaw, M.; Lazar, N.; Sarr, A.; Brochier, T.; Ndiaye, I.; Faye, A.; Sadio, O.; Panfili, J.; Thiaw, O.T.; et al. Resilience of key biological parameters of the Senegalese flat sardinella to overfishing and climate change. *PLoS ONE* **2016**, *11*, e0156143. [[CrossRef](#)]

31. Otegui, M.B.P.; Blankensteyn, A.; Pagliosa, P.R. Population structure, growth and production of *Thoracophelia furcifera* (Polychaeta: Opheliidae) on a sandy beach in Southern Brazil. *Helgol. Mar. Res.* **2012**, *66*, 479–488. [[CrossRef](#)]
32. Strack, H.L. The distribution of Chitons (Polyplacophora) in Greece. *APEX* **1988**, *3*, 67–80.
33. Öztürk, B.; Ergen, Z.; Önen, M. Polyplacophora (Mollusca) from the Aegean coast of Turkey. *Zool. Middle East.* **2000**, *20*, 69–76. [[CrossRef](#)]
34. Barbosa, S.; Byrne, M.; Kelaher, B. Reproductive periodicity of the tropical intertidal chiton *Acanthopleura gemmata* at One Tree Island, Great Barrier Reef, near its southern latitudinal limit. *J. Mar. Biol. Assoc. UK* **2009**, *89*, 405–411. [[CrossRef](#)]
35. Monteiro, A.J.S. Contribuição para o Estudo dos Polyplacophora (Mollusca) da Costa Portuguesa. Relatório de Estágio Curricular. Master's Thesis, University of Lisbon, Lisbon, Portugal, 1982; 159p. Available online: <https://core.ac.uk/download/pdf/12427151.pdf> (accessed on 12 April 2023).
36. Mendonça, V.; Vinagre, C.; Cabral, H.; Silva, A.C.F. Habitat use of inter-tidal chitons—Role of colour polymorphism. *Mar. Ecol.* **2015**, *36*, 1098–1106. [[CrossRef](#)]
37. Schwabe, E. Illustrated summary of chiton terminology (Mollusca, Polyplacophora). *Spixiana* **2010**, *33*, 171–194.
38. Sigwart, J.D.; Green, P.A.; Crofts, S.B. Functional morphology in chitons (Mollusca, Polyplacophora): Influences of environment and ocean acidification. *Mar. Biol.* **2015**, *162*, 2257–2264. [[CrossRef](#)]
39. Avila-Poveda, O.H. Annual Change in Morphometry and in Somatic and Reproductive Indices of Chiton articulatus Adults (Polyplacophora: Chitonidae) from Oaxaca, Mexican Pacific. *Am. Malacol. Bull.* **2013**, *31*, 65–74. [[CrossRef](#)]
40. Chapman, M.G. Aggregation of the littorinid snail *Littorina unifasciata* in New South Wales, Australia. *Mar. Ecol. Prog. Ser.* **1995**, *126*, 191–202. [[CrossRef](#)]
41. Feare, C.J. The adaptive significance of aggregation behaviour in the dogwhelk *Nucella lapillus* (L.). *Oecologia* **1971**, *7*, 117–126. [[CrossRef](#)] [[PubMed](#)]
42. Levings, S.C.; Garrity, S.D. Diel and tidal movement of two co-occurring neritid snails; differences in grazing patterns on a tropical rocky shore. *J. Exp. Mar. Biol. Ecol.* **1983**, *67*, 261–278. [[CrossRef](#)]
43. McKillup, S.C. A behavioural polymorphism in the marine snail *Nassarius pauperatus*: Geographic variation correlated with food availability. *Oecologia* **1983**, *56*, 58–66. [[CrossRef](#)]
44. Glynn, P.W. On the ecology of the Caribbean chitons *Acanthopleura granulata* Gmelin and *Chiton tuberculatus* Linne: Density, mortality, feeding, reproduction and growth. *Smithson. Contrib. Zool.* **1970**, *66*, 1–21. [[CrossRef](#)]
45. Baxter, J.M.; Jones, A.M. Growth and population structure of *Lepidochitona cinereus* (Mollusca: Polyplacophora) infected with *Minchinia chitonis* (Protozoa: Sporozoa) at Easthaven, Scotland. *Mar. Biol.* **1978**, *46*, 305–313. [[CrossRef](#)]
46. Joshua, P.L. Longevity and Growth Rates of the Gumboot Chiton, *Cryptochiton stelleri*, and the Black Leather Chiton, *Katharina tunicata*. *Malacologia* **2012**, *55*, 43–54.
47. Bode, A. Production of the intertidal chiton *Acanthochitona crinita* within a community of *Corallina elongata* (Rhodophyta). *J. Molluscan Stud.* **1989**, *55*, 37–44. [[CrossRef](#)]
48. Crozier, W.J. Growth and duration of life of *Chiton tuberculatus*. *Proc. Natl. Acad. Sci. USA* **1918**, *4*, 322–325. [[CrossRef](#)]
49. Booloottian, R.A. On growth, feeding and reproduction in the chiton *Mopalia muscosa* of Santa Monica Bay. *Helgol. Wiss. Meeresunters.* **1964**, *11*, 186–199.
50. Colomba, M.; Sigwart, J.D.; Renda, W.; Gregorini, A.; Sosso, M.; Dell'Angelo, B. Molecular analysis of *Lepidopleurus cajetanus* (Poli, 1791) (Polyplacophora, Leptochitonidae) from the Mediterranean and near Atlantic. *ZooKeys* **2022**, *1099*, 29–40. [[CrossRef](#)]

Disclaimer/Publisher's Note: The statements, opinions and data contained in all publications are solely those of the individual author(s) and contributor(s) and not of MDPI and/or the editor(s). MDPI and/or the editor(s) disclaim responsibility for any injury to people or property resulting from any ideas, methods, instructions or products referred to in the content.